SCIENCE CHINA
Information Sciences

• LETTER •

November 2026, Vol. 69, Iss. 11, 219306:1–219306:2
https://doi.org/10.1007/s11432-025-5048-4

An ultra-wideband 50-to-110 GHz down-converter integrated with amplifier multiplier chains in 100 nm GaAs for 6G applications

Guomin CHEN[1], Peng CHEN[1*], Zichun ZHENG[1,2], Ziyuan WANG[1], Luqi YU[1], Zhe CHEN[1], Zhengbo JIANG[1,2], Xiao-Wei ZHU[1], Jixin CHEN[1,2], Zhang-Cheng HAO[1,2], Chao YU[1,2] & Wei HONG[1,2*]

[1]*State Key Laboratory of Millimeter Waves, Southeast University, Nanjing 210096, China*
[2]*Purple Mountain Laboratories, Nanjing 211111, China*

Received 15 January 2026/Revised 12 June 2026/Accepted 15 July 2026/Published online 15 October 2026

Citation Chen G M, Chen P, Zheng Z C, et al. An ultra-wideband 50-to-110 GHz down-converter integrated with amplifier multiplier chains in 100 nm GaAs for 6G applications. Sci China Inf Sci, 2026, 69(11): 219306, https://doi.org/10.1007/s11432-025-5048-4

The demand for high-rate, high-reliability communication has increased rapidly with the development of sixth-generation (6G) wireless communication systems. The millimeter-wave (mmWave) frequency band (30 to 300 GHz) has attracted widespread attention due to its wider bandwidth and higher transmission rate. These advantages make mmWave an indispensable spectrum resource for future prominent applications, such as high-speed wireless communication and high-precision radar systems.

This study presents an ultra-wideband 50-to-110 GHz down-converter integrated with amplifier multiplier chains (AMC), as shown in Figure 1(a). The AMC consists of a two-stage tripler and a four-stage amplifier. The two-stage tripler adopts two 2×25 μm transistors, while the four-stage power amplifier (PA) adopts three 2×25 μm transistors and one 4×25 μm transistor. Figure 1(b) illustrates the schematic of the proposed mixer, which employs four 1×10 μm diodes. The floating IF port not only provides high port isolation, but also establishes a forward bias for the diodes.

Analysis of the proposed down-converter. As shown in Figure 1(b), the characteristic impedance and the coupling coefficient can be expressed in (1) and (2),

$$Z_O = \sqrt{Z_{Oe}\times Z_{Oo}}, \tag{1}$$

$$K_c = (Z_{Oe} - Z_{Oo})/(Z_{Oe} + Z_{Oo}), \tag{2}$$

where Z_O, Z_{Oe}, Z_{Oo}, and K_c denote the characteristic impedance, the even-mode impedance, the odd-mode impedance, and the coupling coefficient, respectively. According to [1], the odd-mode impedance Z_{Oo} can be derived from (3),

$$Z_{Oo} = \frac{1}{2}\sqrt{Z_O\times Z_d}, \tag{3}$$

where Z_d denotes the diode impedance. In this wideband mixer design, the characteristic impedance Z_O is selected as 50 Ω. The analytical expression in (3) indicates that the odd-mode impedance Z_{Oo} is related to the diode impedance Z_d, and it reduces down as Z_d decreases. If Z_O remains constant in (1), a reduction in Z_{Oo} will lead to an increase in the even-mode impedance Z_{Oe}. According to (2), the coupling coefficient K_c will increase correspondingly. As per [2], the enhancement in K_c can enlarge the operational bandwidth, whilst simultaneously reducing the conversion loss. Therefore, when determining the optimal diode impedance, a trade-off between the bandwidth and the conversion loss should be carefully considered. The diode impedance Z_d is governed by the voltage applied across its terminals. The real part of the diode impedance is given as follows:

$$\mathrm{Re}(Z_d) = R_d + \frac{nkT}{qI_O}, \tag{4}$$

$$I_O = I_s\left[\exp\left(\frac{qV_O}{nkT}\right) - 1\right], \tag{5}$$

where T is the absolute temperature, k is the Boltzmann constant, n is the ideality factor, q is the elementary charge, I_O is the diode current, and R_d is a parameter related to the physical dimensions of the diode. Moreover, V_O signifies the voltage applied across the diode, and I_s represents the saturation current, respectively. It is worth noting that the real part of the diode impedance Z_d can be tuned by varying the voltage that is applied across it. Based on (1)–(3), we can see that the odd-mode impedance Z_{Oo}, the characteristic impedance Z_O and the coupling coefficient K_c will change in relation to Z_d. In view of this, we can optimize the coupling coefficient K_c, and so as to make a good trade-off between the bandwidth and the conversion loss.

To optimize the overall performance of the wideband mixer, the coupling coefficient K_c, the conversion loss and the return loss S_{11} at the radio frequency (RF) port versus frequency are investigated in Figure 1(c). When varying V_O from 0.8 to 1.1 V, K_c rises up and S_{11} reduces down, indicating the enlargement of the RF bandwidth. In the meantime, the conversion loss becomes worse,

* Corresponding author (email: pchen@seu.edu.cn, weihong@seu.edu.cn)

© Science China Press 2026

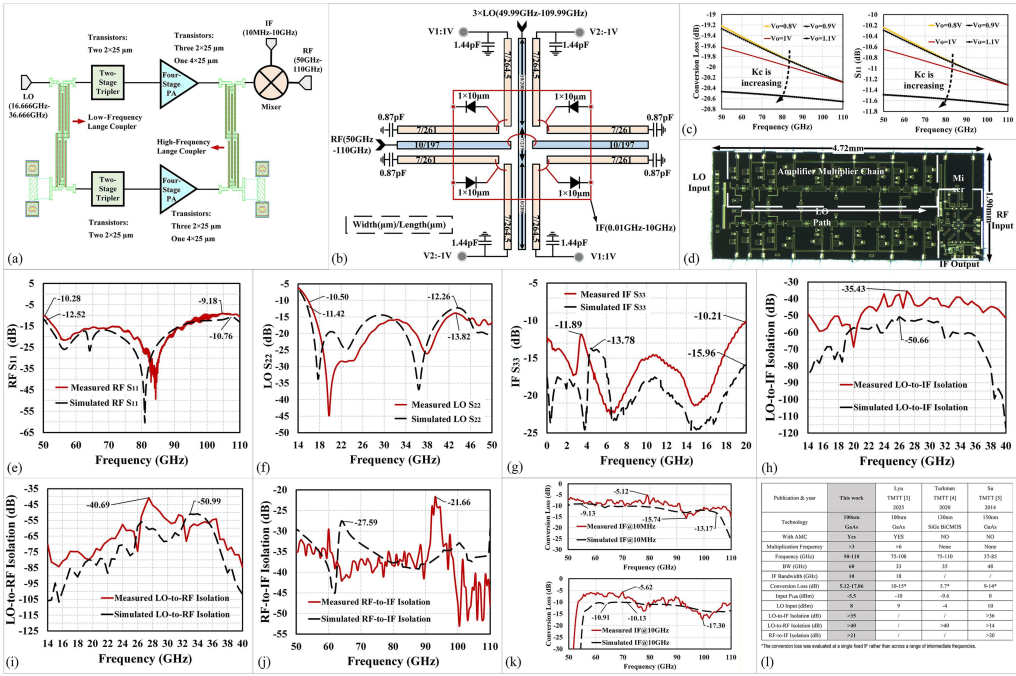


Figure 1 (a) The simplified schematic; (b) schematic of the wideband star mixer; (c) the conversion loss and the return loss in relation to the coupling coefficient K_c; (d) the fabricated MMIC down-converter; (e) the RF port (S11); (f) the LO port (S22); (g) the IF port (S33); (h) the LO-to-IF isolation; (i) the LO-to-RF isolation; (j) the RF-to-IF isolation; (k) measured and simulated conversion loss; (l) comparison to prior-art mmWave mixers.

which is as expected from the above analysis. Taking account of the trade-off between the conversion loss and the RF bandwidth, the optimum voltage $V_O = 1$ V is applied for the diodes. The load capacitance can be determined through optimizing the return loss and the conversion loss. Although lumped capacitors are more affected by process variation than transmission line-based capacitors, they are employed to minimize the overall footprint.

Experimental verification. The micrograph of the fabricated MMIC down-converter is shown in Figure 1(d), with an occupied mask area of 4.72 mm × 1.90 mm.

In small-signal condition, the measured and simulated return loss of the RF port (S_{11}), local oscillator (LO) port (S_{22}) and intermediate frequency (IF) port (S_{33}) are evaluated. The measured S_{11} remains below −9.18 dB over 50 to 110 GHz, and below −10 dB from 50 to 98.6 GHz, as shown in Figure 1(e). The simulated S_{11} is below −10 dB across the entire band, which is similar to the measured data. Additionally, Figures 1(f) and (g) show the return loss of the LO and IF ports, respectively. The LO port achieves a measured S_{22} below −10 dB across 15.9 to 50 GHz, and the simulated S_{22} is below −10 dB from 15.3 to 50 GHz, which shows a similar trend. Although the measured S_{33} is less than −10 dB from DC to 20 GHz, the effective IF bandwidth must also be determined based on the conversion loss.

Figures 1(h)–(j) show the isolation of the three ports. Measured results indicate that the isolation levels are better than −35.43 dB (LO-to-IF isolation), −40.69 dB (LO-to-RF isolation), and −21.66 dB (RF-to-IF isolation) within the specified bandwidths, while simulated results demonstrate the isolation margins of −50.66, −50.99, and −27.59 dB, respectively. The LO-to-RF isolation particularly exhibits outstanding isolation performance. The experimental DC power consumption versus the LO frequency falls within 0.97 to 1.09 W, which is close to the simulated results of 0.97 to 1.00 W. The differences between the measured and simulated results are mainly ascribed to the accuracy between the fabrication process and the design kit used in simulation.

Figure 1(k) presents the conversion loss of the MMIC down-converter from 50 to 110 GHz. To characterize the conversion loss and its flatness across the RF frequency, the IF was fixed, while the LO frequency was changed in accordance with the relationship LO = RF-IF. When the IF is fixed at 10 MHz, the measured conversion loss ranges from −5.12 to −15.74 dB across the band. When the IF is set at 10 GHz, the measured conversion loss ranges from −5.62 to −17.30 dB over 55.5 to 110 GHz. It is noteworthy that when the RF frequency approaches 50 GHz, the measured conversion loss is degraded significantly. This is because the LO chain is out of its operation frequency and fails to activate the diodes in the mixer. Overall, the conversion loss remains low with acceptable fluctuations over 50 to 110 GHz.

Figure 1(l) shows the comparison of the proposed down-converter against the mixers reported in [3–5]. Compared to the state-of-the-art, it achieves the widest operation bandwidth with a competitive conversion loss in 100 nm GaAs.

Acknowledgements This work was supported in part by Top-Ten Technological Projects for Hunan Province in 2025 (Grant No. 2025QK1009) and National Natural Science Foundation of China (Grant Nos. 62188102, 62131008).

References

1 Zhang A, Gao J. Characterization of GaN Schottky barrier diode for multifinger application. IEEE Microw Wireless Tech Lett, 2025, 35: 1586–1589
2 Lien C H, Wang C H, Lin C S, et al. Analysis and design of reduced-size marchand rat-race hybrid for millimeter-wave compact balanced mixers in 130-nm CMOS process. IEEE Trans Microwave Theor Techn, 2009, 57: 1966–1977
3 Lyu W, Zhou P, Chen J, et al. A W-band bidirectional RF front-end in 0.1-μm GaAs pHEMT technology. IEEE Trans Microwave Theor Techn, 2025, 73: 8757–8767
4 Turkmen E, Gurbuz Y. A SiGe BiCMOS W-band single-chip frequency extension module for VNAs. IEEE Trans Microwave Theor Techn, 2020, 68: 211–221
5 Su C C, Lin C M, Hung S H, et al. Analysis of three-conductor coupled-line 180° hybrid for single-balanced subharmonic mixer design in 0.15-μm pHEMT technology. IEEE Trans Microwave Theor Techn, 2014, 62: 2405–2414